BIOCHEMISTRY
including biophysical chemistry & molecular biology

Article

pubs.acs.org/biochemistry



# Secreted Amyloid β-Proteins in a Cell Culture Model Include N-Terminally Extended Peptides That Impair Synaptic Plasticity

Alfred T. Welzel,[†,#] John E. Maggio,[‡,§,#] Ganesh M. Shankar,[‡,#] Donald E. Walker,[∥] Beth L. Ostaszewski,[‡] Shaomin Li,[‡] Igor Klyubin,[⊥] Michael J. Rowan,[⊥] Peter Seubert,[∥] Dominic M. Walsh,*[,†,‡] and Dennis J. Selkoe*[,‡]

[†]Laboratory for Neurodegenerative Research, Conway Institute of Biomedical and Biomolecular Research, University College Dublin, Belfield, Dublin 4, Republic of Ireland

[‡]Department of Neurology, Harvard Medical School and Center for Neurologic Diseases, Brigham and Women's Hospital, Boston, Massachusetts 02115, United States

[§]Department of Pharmacology and Cell Biophysics, University of Cincinnati College of Medicine, Cincinnati, Ohio 45267, United States

[∥]Elan Pharmaceuticals, South San Francisco, California 94080, United States

[⊥]Institute of Neuroscience and Departments of Pharmacology and Therapeutics, Trinity College, Dublin 2, Republic of Ireland

Supporting Information

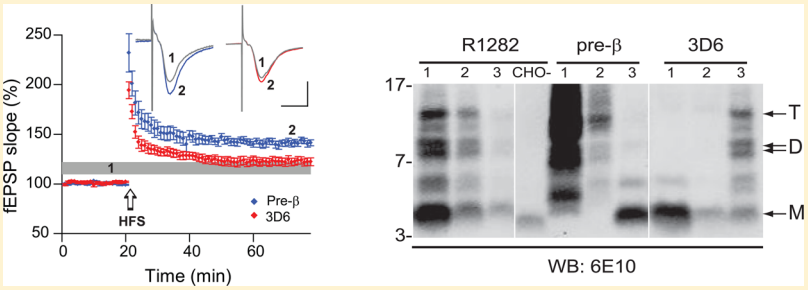


**ABSTRACT:** Evidence for a central role of amyloid β-protein (Aβ) in the genesis of Alzheimer's disease (AD) has led to advanced human trials of Aβ-lowering agents. The "amyloid hypothesis" of AD postulates deleterious effects of small, soluble forms of Aβ on synaptic form and function. Because selectively targeting synaptotoxic forms of soluble Aβ could be therapeutically advantageous, it is important to understand the full range of soluble Aβ derivatives. We previously described a Chinese hamster ovary (CHO) cell line (7PA2 cells) that stably expresses mutant human amyloid precursor protein (APP). Here, we extend this work by purifying an sodium dodecyl sulfate (SDS)-stable, ∼8 kDa Aβ species from the 7PA2 medium. Mass spectrometry confirmed its identity as a noncovalently bonded Aβ40 homodimer that impaired hippocampal long-term potentiation (LTP) in vivo. We further report the detection of Aβ-containing fragments of APP in the 7PA2 medium that extend N-terminal from Asp1 of Aβ. These N-terminally extended Aβ-containing monomeric fragments are distinct from soluble Aβ oligomers formed from Aβ1-40/42 monomers and are bioactive synaptotoxins secreted by 7PA2 cells. Importantly, decreasing β-secretase processing of APP elevated these alternative synaptotoxic APP fragments. We conclude that certain synaptotoxic Aβ-containing species can arise from APP processing events N-terminal to the classical β-secretase cleavage site.

Rapid progress in the mechanistic study of several human neurodegenerative diseases has revealed a potentially common mode of pathogenesis: that small, soluble oligomers of misfolded proteins, rather than much larger, insoluble fibrous deposits, play the principal role in initiating and propagating neuronal injury. Examples of this reinterpretation have emerged from the study of α-synuclein in Parkinson's disease, huntingtin in Huntington's disease, and amyloid β-protein (Aβ) in Alzheimer's disease (AD). Studies of the latter disorder have accrued the most evidence for the pathogenic oligomer hypothesis of neurodegeneration. Soluble oligomers of Aβ ranging from dimers to dodecamers and somewhat larger assemblies have been shown to impair synaptic structure and function in both cell culture and animal models (for example, refs 1−7).

Because therapeutic approaches to AD and other protein misfolding disorders could benefit from selectively targeting soluble neurotoxic protein oligomers, it has become increasingly important to identify the full range of pathogenic forms of the respective proteins. In 1995, we reported the first example of a cell culture model (7PA2 cells: Chinese hamster ovary (CHO) cells stably expressing Val717Phe human amyloid protein precursor (APP)) in which the secretion of 4 kDa Aβ monomers was accompanied by the secretion of ∼8.5−12.5 kDa Aβ-immunoreactive

**Received:** March 11, 2014
**Revised:** May 19, 2014
**Published:** May 19, 2014

   dx.doi.org/10.1021/bi5003053 | *Biochemistry* 2014, 53, 3908−3921

species that, by immunochemical analysis and radiosequencing, had the properties of dimers and trimers of Aβ.[8] Subsequently, we and others showed that the latter larger species (but not the monomers) released by the 7PA2 cells could disrupt hippocampal long-term potentiation (LTP),[2,4,9] decrease dendritic spine density,[6,10] inhibit synaptic vesicle recycling,[11] facilitate hippocampal long-term depression,[12] and impair the memory of a learned behavior in adult rodents.[13−16]

Despite this evidence that low-n Aβ oligomers in the 7PA2 cell conditioned medium (CM) produce multiple neural effects analogous to some key features of AD, the precise molecular identity of the oligomers has not been established. This is in large part due to the technical difficulties in purifying the low (subnanomolar) quantities of soluble Aβ oligomers in the CM of these cells and then successfully ionizing the hydrophobic oligomers during mass spectrometry in order to identify their exact masses. In the current work, we have used a range of biochemical, immunochemical, and mass spectrometric methods to analyze the Aβ species produced in this highly useful and rather widely used cell culture model. Two principal findings have emerged: (1) that the ∼8 kDa species has a mass indicating that it is a noncovalently bonded dimer of Aβ, as originally hypothesized, and (2) that there are also Aβ-immunoreactive species in the CM which represent Aβ monomers that bear sequences which are N-terminally extended (NTE) beyond the conventional Aβ Asp1 start site. We designate these novel species as NTE-Aβ. We show that while both authentic noncovalent dimers and the NTE-Aβ peptides can impair synaptic plasticity in the hippocampus, NTE-Aβ species are much more abundant than Aβ dimers in the particular CHO cell line we employ. Importantly, treatment of the cells with pharmacological inhibitors of β-secretase caused increased processing of APP via this alternative pathway, producing more synaptotoxic NTE-Aβ peptides. Our findings extend the range of Aβ-containing APP peptides that are capable of impairing synaptic function and suggest that synaptotoxicity can arise from APP processing events in addition to the classical β- and γ-secretase cleavages that produce Aβ.

## EXPERIMENTAL PROCEDURES

**Reagents.** Unless otherwise stated, all chemicals and reagents were purchased from Sigma (Sigma-Aldrich, St. Louis, MO) and were of the highest purity available. Synthetic Aβ(1−40) was synthesized and purified by Dr. James I. Elliott at Yale University and was >99% pure. The β-secretase inhibitors *N*-(1*S*,2*R*)-1-benzyl-3-(cyclopropylamino)-2-hydroxypropyl)-5-(methyl-(methylsulfonyl)amino-*N*′-((1*R*)-1-phenylethyl)isophthalamide (Compound IV) and H-EVNstatineVAEF-NH2 (Compound III) were from Calbiochem (Billerica, MA). The γ-secretase inhibitors (2*S*)-2-{[(3,5-difluorophenyl)acetyl]amino}-*N*-[(3*S*)-1-methyl-2-oxo-5-phenyl-2,3-dihydro-1*H*-1,4-benzodiazepin-3-yl]propanamide (Compound E) and *N*-[*N*-(3,5-difluorophenacetyl)-L-alanyl]-*S*-phenylglycine *tert*-butyl ester (DAPT) were gifts of Dr. Mike Wolfe (Center for Neurologic Diseases).

**7PA2 and Flp-In CHO Cell Lines Bearing Mutant Human APP.** Cell culture media, fetal bovine serum (FBS), and media supplements were from Invitrogen. Naïve, untransfected CHO cells were grown in Dulbecco's modified Eagle's medium (DMEM) containing 10% fetal bovine serum, 100 units/mL penicillin, 100 μg/mL streptomycin, and 2 mM L-glutamine. CHO cells stably transfected with human $APP_{751}$ bearing the V717F mutation (7PA2 cells) were grown in CHO medium plus G418 (200 μg/mL). Isogenic CHO cell lines stably expressing human $APP_{695}$ with the wild type sequence or bearing one of the following coding changes (i) Lys595Asn, (ii) Met596Leu, or (iii) Met596Val were generated using the Flp-In (Invitrogen). Briefly, naïve CHO cells were transfected with the pFRT/lacZeo vector using lipofectamine 2000, and cells stably expressing β-galactosidase selected in medium supplemented with zeocin (0.1 mg/mL) and a clonal cell line (referred to as pCHO-) were isolated by limiting dilution. DNA encoding $APP_{695}$ was cloned into pcDNA5/FRT and PCR site-directed mutagenesis used to introduce single base changes resulting in desired mutations at $APP_{595}$ or $APP_{596}$. The pOG44 plasmid and pcDNA5/FRT-APP vectors were cotransfected into the pCHO- host cell line. Flp-In cells stably expressing human APP were selected using hygromycin (0.5 mg/mL) and confirmed to lack β-galactosidase activity and to express human APP.

For conditioning, cells were allowed to reach 90−100% confluency, washed once with unsupplemented DMEM (5 mL), and incubated for ∼15 h in DMEM (5 mL). CM was collected and spun at 200*g* and 4 °C for 10 min to remove cellular debris, the upper 4.5 mL removed, and centrifuged a second time (3000*g*, 10 min, 4 °C) to pellet particulate debris. To inhibit proteolysis, Ethylenediaminetetraacetic acid (EDTA) was added to achieve a final concentration of 50 mM and CM used immediately or stored at −80 °C pending use. Storing CM at −80 °C does not alter the profile of 6E10-reactive material immunoprecipitated by either AW8 or R1282.

**Antibodies.** The antibodies used in this study are listed in Table 1.

**Immunoprecipitation (IP) of Cell Medium.** Samples were first incubated with 30 μL of a 1:1 mixture of protein A sepharose

**Table 1. Anti-APP Monoclonal and Polyclonal Antibodies**[a]

| name | monoclonal/polyclonal | epitope | source/ref | Wblot dil./conc. | IP dil./conc. |
|---|---|---|---|---|---|
| 8E5 | monoclonal | APP444-592 | Elan[45] | N/A | 5 μg/mL |
| Rita | polyclonal | APP527-540 | Selkoe laboratory[8] | N/A | 1:50 |
| Pre-β | polyclonal | APP577-596 | Selkoe laboratory[8] | 1:500 | 1:50 |
| 1G6 | monoclonal | APP573-576 | Covance | N/A | 10 μg/mL |
| 3D6 | monoclonal | Aβ1−5(Asp1) | Elan | 1 μg/mL | 5 μg/mL |
| 82E1 | monoclonal | Aβ1−5(Asp1) | immunobiological laboratories | N/A | 10 μg/mL |
| 6E10 | monoclonal | Aβ6−10 | Signet[31] | 1 μg/mL | 5 μg/mL |
| 4G8 | monoclonal | Aβ17−24 | Signet[46] | 1 μg/mL | 5 μg/mL |
| 2G3 | monoclonal | Aβ31−40 | Elan[47] | 2 μg/mL | 5 μg/mL |
| 21F12 | monoclonal | Aβ33−42 | Elan[47] | 2 μg/mL | 5 μg/mL |
| R1282 | polyclonal | raised to Aβ1−40 | Selkoe laboratory[48] | N/A | 1:100 |
| AW8 | polyclonal | raised to Aβ1−42 | Walsh laboratory[49] | N/A | 1:100 |
| C8 | polyclonal | to residues $APP_{676-695}$ | Selkoe laboratory[48] | 1:1000 | 1:50 |

[a]APP numbering is based on the 695 isoform. Dil. = dilution; conc. = concentration; and N/A = not applicable.


dx.doi.org/10.1021/bi5003053 | *Biochemistry* 2014, 53, 3908−3921

(PAS) and protein G agarose (PAG) (Roche, Mannheim, Germany) for 6 h at 4 °C. Beads were sedimented by centrifugation at 3500*g* for 10 min and the cleared supernatant incubated with appropriate antibody (Table 1) plus 30 μL of PAS/PGA and rocked on a nutator for 12−14 h at 4 °C. Antibody−antigen complexes were collected and pellets washed as described previously.[17]

**Polyacrylamide Gel Electrophoresis (PAGE) and Western Blotting.** Immunoprecipitated (IP'd) proteins were released from the antibody complex by heating at 100 °C in 2× sample buffer and then electrophoresed on either hand poured 16% polyacrylamide tris-tricine gels or precast 4−12% polyacrylamide NuPAGE bis-tris gels from Invitrogen.[18] Proteins were transferred onto nitrocellulose membranes at 400 mA for 2 h and then microwaved in 200 mL of PBS at 800 W for 90 s ×2. Membranes were blocked for 1 h at room temperature in TBST containing 5% (w/v) skim milk and then incubated with antibody (Table 1) for 1 h at room temperature or 12 h at 4 °C. Membranes were washed 6 times for 10 min with PBS containing 0.05% (v/v) Tween 20 (PBST) and then incubated with goat antimouse infrared 800 antibody or antirabbit 800 infrared antibody (Rockland, Gilbertville, PA) diluted in PBST containing 0.01% (w/v) SDS. Immunoreactive bands were visualized using a Li-COR Odyssey infrared imaging system (Li-COR, Lincoln, NE).

**Western Blot Analysis of Size-Exclusion Chromatography (SEC) Isolated 7PA2 Fractions.** Fourteen milliliter aliquots of 7PA2 CM were concentrated ∼10-fold (1.4 mL) using Centriprep Ultracel YM-3 filters (Millipore, Carrigtwohill, Co. Cork, Ireland) and concentrates used immediately or stored at 4 °C for ≤24 h prior to use. One milliliter of 10-fold concentrated 7PA2 CM was chromatographed on a Superdex 75 10/300 GL (Amersham Biosciences AB, Uppsala, Sweden) eluted in 50 mM ammonium acetate at pH 8.5 at a flow-rate of 0.8 mL/min using an AKTA purifier (GE Healthcare Biosciences AB, Uppsala, Sweden). One milliliter fractions were collected, lyophilized, then resuspended in 20 μL of sample buffer and used for Western blotting.

**Purification of Aβ from 7PA2 CM.** After considerable experimentation, a 4-step purification strategy was implemented (Figures 2 and 3). The first step involved the removal of soluble APP (APPs) from 7PA2 CM using DE23 cellulose. This was achieved by adding DE23 cellulose (0.5 mL settled volume in DMEM) to 5 mL of 7PA2 CM and gently rocking for 30 min at room temperature. The APP-depleted CM was separated from the DE23 cellulose using a 0.2 μM stericup vacuum filter unit (Millipore, Carrigtwohill, Co. Cork, Ireland). Thereafter, the supernatant was incubated with a 60 μL suspension of either (1) AW8 conjugated to PAS or (2) 2G3/21F12 conjugated to PGA (Figure 2) and gently mixed for 12 h at 4 °C. Beads were sedimented by centrifugation (3500*g* for 10 min at 4 °C) and washed using STEN buffers.[17] Bound proteins were eluted by resuspending the beads in 100 mM $NH_4OH$ (200 μL) and vortex mixing for 2 min. The supernatant was then transferred to a clean tube, snap frozen, and lyophilized. Samples were resuspended in 20 mM ammonium acetate at pH 8.5 (buffer A, 5 mL) and used for ligand affinity chromatography. Briefly, 30 mg of methanol-washed dry KLVFFAE-Ac-HN-$(CH_2)$3-CPG beads (Senexis Limited, Cambridge, UK) was added to the immunopurified 7PA2 preparation and incubated with gentle agitation for 30 min. Beads were recovered by centrifugation (3000*g*, 5 min) and washed with 5% acetonitrile in buffer A (5 mL × 3) and then eluted using 20% acetonitrile in buffer A (5 mL). The sample was then lyophilized and immediately prior to SEC dissolved in 50 mM ammonium acetate at pH 8.5 (1 mL), and applied to a Superdex 75 column and eluted as describe above. Half milliliter fractions were collected, an aliquot taken for LTP experiments, and the remainder lyophilized and used for Western blot and silver stain analysis.

**Silver Staining and In-Gel Digestion of Excised SDS−Polyacrylamide Bands for Liquid Chromatography (LC) MALDI-TOF.** Electrophoresed proteins were detected using the protocol of Shevchenko et al.[19] and bands of interest excised using a clean razor blade. Excised bands were cut into ∼1 mm pieces and silver stain removed by incubating the pieces in 500 μL of a 1:1 mixture of Silverquest Silver Stain Kit destaining reagents A and B (Invitrogen, Carlsbad, CA, USA) for 3 h. Gel pieces were washed briefly with distilled water (500 μL × 2) and then 50 mM ammonium bicarbonate in 50% ACN (500 μL × 2) for 30 min. Gel pieces were completely dehydrated by incubation in 100% ACN (500 μL) for 20 min and samples reduced to dryness in a vacuum centrifuge.

For trypsin digests, 200 ng of porcine trypsin (20 μL, Promega, Madison, WI, USA) was used to rehydrate the gel pieces. The suspension was incubated for 3 h at 37 °C, and the reaction was stopped by the addition of 1% formic acid (10 μL). For LysC digestions, 200 ng of endoproteinase LysC (20 μL) was used to rehydrate the gel pieces. Digests were incubated overnight at 30 °C and the reaction stopped with 1% formic acid (10 μL). Samples were then bath sonicated for 30 min and 15 μL injected onto a 75 μm × 30 cm column (New Objective, Woburn, MA, USA) packed with a Magic C18 AQ stationary phase (Michrom Biosciences, Auburn, CA, USA) connected to a Michrom Magic 2002 capillary HPLC (Michrom Biosciences, Auburn, CA, USA). Samples were eluted using a linear gradient of 0.1% aqueous formic acid to 50% acetonitrile containing 0.1% formic over 50 min. Peaks corresponding to tryptic peptides were subjected to nanospray ionization and analyzed using a Quadrupole-Time of Flight mass spectrometer (QStar, Thermo Electron Corp, San Jose, CA, USA).

**In Vivo LTP.** Adult male Wistar rats were anesthetized with an intraperitoneal injection of urethane (1.5 g/kg), and a cannula was implanted in the lateral cerebral ventricle 1 mm lateral to the midline and 4 mm below the surface of the dura mater. Single pathway recordings of excitatory post-synaptic potentials (EPSPs) were recorded from the stratum radiatum in the CA1 area of the dorsal hippocampus in response to stimulation of the ipsilateral Schaffer collateral/commissural pathway.[4] EPSPs were evoked at a frequency of 0.033 Hz. Test EPSPs were stimulated to give 50% of the maximum amplitude. High frequency stimulation (HFS) to induce LTP consisted of 10 trains of 20 stimuli with an intertrain interval of 2 s and an interstimulus interval of 5 ms (200 Hz). During HFS, the stimulation intensity was adjusted to produce an EPSP ≥75% of the maximum amplitude. Intracerebroventricular (icv) injection of the sample was made 10 min prior to HFS and solutions injected at ∼5 μL per min (total volume 10 μL).

**Two-Dimensional Gel Electrophoresis of 7PA2 CM SEC Isolated Fractions.** 7PA2 CM was concentrated ∼10-fold using a Centriprep Ultracel YM-3 filter and then used for SEC as in Figures 1B and 4A. Fractions 8, 9, and 10 were pooled to a give a preparation rich in Aβ immunoreactive species of masses between ∼14 and 4 kDa. This material was then lyophilized, reconstituted in 125 μL of rehydration buffer (7 M urea, 2 M thiourea, 2% (w/v) CHAPS, and 0.2% (v/v) Pharmalyte, 3−10) (GE Healthcare) and electrofocused on immobilized pH gradient

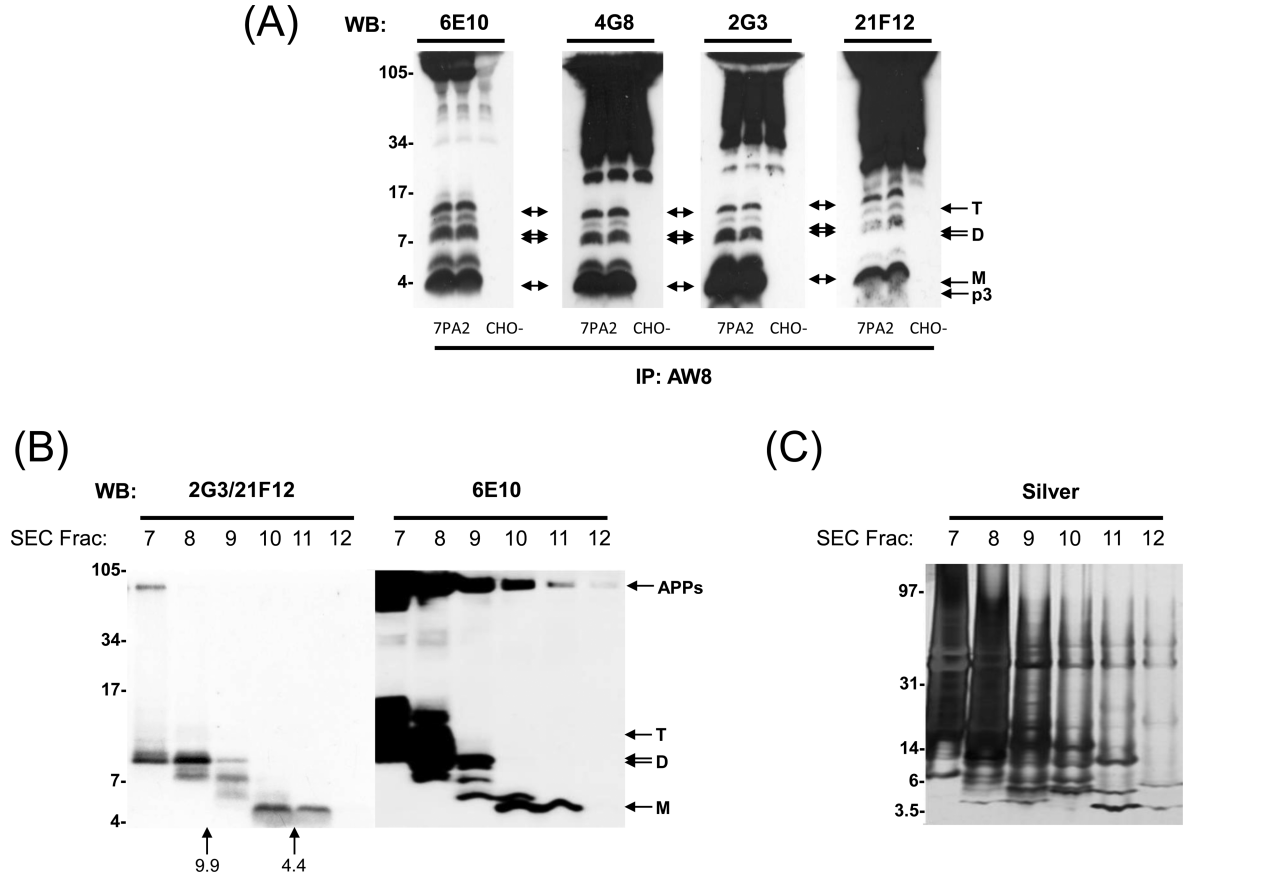


**Figure 1.** 7PA2 conditioned medium contains A$\beta$-immunoreactive species which migrate on SDS−PAGE with molecular weights consistent for A$\beta$ monomer, dimers, and trimers. (A) Conditioned medium from 7PA2 and untransfected CHO cells (3 mL per lane) were IP'd with the pan anti-A$\beta$ polyclonal antibody, AW8, and then Western blotted using the antibodies indicated at the top of each panel. M, D, and T denote the position where putative A$\beta$ monomer, dimer, and trimer species migrate. p3 refers to the well-known ~3 kDa product of $\alpha$-/$\gamma$-secretase cleavage that is detected by 2G3 and 21F12. (B and C) 1 mL of 10× concentrated 7PA2 CM was chromatographed on a Superdex 75 column, fractions collected, lyophilized, and used for SDS−PAGE and Western blotting (B) or silver stain (C). The migrations of SDS−PAGE molecular weight standards (in kDa) are indicated on the left, and elution of linear dextran SEC standards of 9.9 and 4.4 kDa are indicated by vertical arrows.

(IPG) strips (pH 4−7) (GE Healthcare). After focusing was complete, IPG strips were incubated with 6 mL of SDS-equilibration buffer (6 M urea, 50 mM Tris, 2% (w/v) SDS, 30% (v/v) glycerol, and 0.01% (w/v) phenol red) in a 15 mL tube for 15 min and then placed on top of a 4−12% bis-tris gel. The IPG gel was secured in position with agarose dissolved in running buffer so that the IPG gel could be in contact the stacking gel. Molecular weight markers were loaded in a well next to the IPG strip. Gels were electrophoresed at 50 V for 10 min, and then the voltage was increased to 120 V for 2.5 h. The IPG strip was removed from the top of the gel and proteins in the gel transferred onto nitrocellulose and Western blotted using 6E10 as described above and in Table 1.

**Western Blot and Cyanogen Bromide Cleavage Analysis of SEC-Isolated 7PA2 Fractions.** Concentrated 7PA2 CM was chromatographed on a Superdex 75 column and fractions collected as described above. Then fractions 8 and 9 (designated as Oligo), and fraction 10 (designated as Mono) were lyophilized in separate microcentrifuge tubes. Lyophilizates were dissolved in 30 $\mu$L of 70% formic acid ±0.1 M CNBr. Tubes were capped under nitrogen, vortexed, and then spun gently to move solutions to the bottom of the tubes. Samples were incubated in the dark at room temperature for 20 h, after which 330 $\mu$L of Milli-Q water was added and the contents frozen and lyophilized. Dry samples were reconstituted in 2× sample buffer sample, electrophoresed on 12% polyacrylamide bis-tris gels, and proteins transferred onto nitrocellulose and Western blotted as described above.

**In Vitro LTP.** Brains from ~6−8 week old C57BL/6x129 mice were quickly removed and submerged in ice-cold oxygenated cutting solution.[12] Transverse slices (350 $\mu$m thick) were cut with a vibroslicer from the middle portion of each hippocampus. Slices were then incubated in artificial cerebrospinal fluid (ACSF), subsequently transferred to a recording chamber, and continuously perfused at RT (~24 °C) with 9 mL of ACSF saturated with 95% $O_2$ and 5% $CO_2$. Field EPSPs (fEPSP) were recorded in the CA1 region of hippocampus induced by test stimuli at 0.05 Hz with an intensity that elicited an fEPSP amplitude of 40−50% of maximum. Once a stable baseline was achieved, 1 mL of test medium was added to the perfusion bath and the slice incubated for a further 20 min prior to stimulation. Thereafter, LTP was induced by two consecutive trains (1 s) of stimuli at 100 Hz.

## RESULTS

**Medium Conditioned by 7PA2 Cells Contain A$\beta$-Immunoreactive Species Which Migrate on SDS−PAGE and Elute from Size Exclusion with Molecular Weights Consistent with A$\beta$ Monomers, Dimers, and Trimers.** 7PA2 cells stably express human $APP_{751}$ bearing the V717F familial AD mutation and secrete significant amounts of APP metabolites into their


dx.doi.org/10.1021/bi5003053 | Biochemistry 2014, 53, 3908−3921

medium.[2,8,21] Since the total amount of ELISA-detectable Aβ secreted by these cells is in the low to subnanomolar range,[22] immunoprecipitation (IP) with polyclonal pan anti-Aβ antibodies has been widely used to concentrate and facilitate the detection of 7PA2 Aβ (reviewed in ref 18). Here, we show that when 7PA2 CM is IP'd with AW8 and Western blotted with anti-Aβ monoclonal antibodies, a ladder of bands between ∼3 and ∼16 kDa is detected (Figure 1A). Specifically, AW8 captures ∼4.5, 5.8, 8.5/9 (a doublet) and ∼12.5 kDa species that react with N-terminal (6E10), midregion (4G8), and C-terminal (2G3 and 21F12) anti-Aβ antibodies (Figure 1A). It should be noted that in these IP/Western blot experiments, nonspecific high molecular weight bands are observed in the CM of both 7PA2 and CHO cells, most of which are due to the detection of the IP antibody by the secondary antibody used for immunoblotting.

Importantly, when 7PA2 CM is subjected to native SEC, Aβ-immunoreactive species elute with molecular weights consistent with estimates made using denaturing SDS−PAGE (Figure 1B), that is, with sizes indicative of Aβ monomer, dimers, and trimers. In prior studies, we found that the plasticity-disrupting activity of 7PA2 CM was present in SEC fractions that contain the ∼8.5/9 and ∼12.5 kDa species.[4,9,13] However, silver staining of the same SEC fractions demonstrates that the proteins recognized by anti-Aβ antibodies contribute only a small portion of the total proteins present (Figure 1C). Thus, in order to definitively ascribe bioactivity to the ∼8.5/9 and ∼12.5 kDa Aβ-reactive species, we sought to purify these species to homogeneity, test their effect on LTP, and determine their primary sequence by mass spectrometry.

**Purification of an SDS-Stable Aβ Dimer from the 7PA2 Conditioned Medium.** In order to identify methods suitable for purifying Aβ species from 7PA2 CM, numerous chromatographies were tested for their ability to bind Aβ and remove extraneous proteins, as assessed by IP/WB and qualitative silver staining. The chromatographies tested included (1) hydrophobic interaction, (2) diol normal phase, (3) PCM cation exchange, (4) C18 reverse-phase, (5) MonoQ anion-exchange, (6) DE23 anion-exchange, (7) immunoaffinity capture, and (8) ligand-binding. The first three chomatographies showed little affinity for Aβ and were not investigated further, and various combinations of C18, anion-exchange, immunoaffinity, and ligand binding were tested. After extensive testing, the four-step protocol outlined in Figure 2A produced the best yield and highest purity of Aβ species and comprised the (1) removal of large amounts of soluble APP (APPs); (2) use of immunoaffinity methods to enrich Aβ species; (3) use of a peptide ligand (KLVFFAE) as a homotypic Aβ affinity reagent; (4) separation of the resultant Aβ assemblies by size-exclusion chromatography; and then electrophoresis of the SEC fractions on SDS−PAGE. Step 2 used either protein-A-sepharose-coupled AW8 antiserum (AW8-PAS) (Figure 2) or protein-G-agarose-coupled 2G3/21F12 (2G3/21F12-PGA), both of which yielded similar results (compare Figure 2B and C to D and E). 6E10 Western blotting of material purified as outlined in Figure 2A revealed that the ∼4.5 kDa monomer and the ∼8.5 kDa dimer elute in SEC fractions 16−22 and 14−21, respectively, with peak levels of monomers and dimers in fractions 20 and 17, respectively (Figure 2B). Silver staining of these fractions showed peaks of total protein tracking with immunoreactivity (Figure 2C). Similar results were obtained when 2G3/21F12-PGA was used as the immunoaffinity reagent (Figure 2E). Compared to the greater amounts of Aβ purified by AW8-PAS, the ∼4.5 and ∼8.5 kDa species purified by 2G3/21F12-PGA eluted in a smaller number of SEC fractions: 16−17 and 18−22 for the monomer and dimer, respectively.

Each purification started with 50 mL of CM, and 30% of the final SEC fractions were used for the 6E10 immunoblot. Comparison of starting material and purified material indicates the excellent recovery of the monomer, reasonable recovery of the dimer, and no recovery of the trimer.

**Mass Spectrometry of Purified, Cell-Secreted Aβ Indicates the Presence of SDS-Stable Dimers Composed of Two Unmodified Aβ1−40 Monomers.** The ∼4.5 and ∼8.5 kDa species purified from 7PA2 CM as described in Figure 2 were excised from silver-stained polyacrylamide gels, digested with proteases, and used for matrix-assisted laser desorption/ionization time-of-flight mass spectrometry (MALDI-TOF MS). Liquid chromatography-separated tryptic digests of the ∼4.5 kDa monomer band produced peaks with masses consistent with the expected products of trypsin-cleaved Aβ1−40, that is, Aβ1−5, Aβ6−16, Aβ17−28, and Aβ29−40 (with a methionine35 sulfoxide) (Figure 3A,B; Table 2). These results are in keeping with the fact that Aβ1−40 is the predominant Aβ peptide secreted by 7PA2 cells and that peptides with other C-termini are only present at low levels.[21,23] Importantly, tryptic digests of the ∼8.5 kDa band also produced mass peaks corresponding to Aβ fragments 1−5, 17−28, and 29−40 (methionine-sulfoxide) (Figure 3C; Table 2); however, Aβ6−16 was not identified. Detection of the 6−16 fragment is crucial to discriminate between noncovalently and covalently cross-linked dimers. Under certain circumstances, Aβ can be induced to form covalently linked dimers, either by phenolic coupling of tyrosine10[24−26] or by formation of an intermolecular isopeptide bond between Lys16 and Gln15.[27,28] In both these types of cross-linked dimers, tryptic digestion would not yield the 6−16 fragment released from the Aβ monomer but instead would give rise to much larger fragments. The failure to detect Aβ6−16 from trypsin digests of the ∼8.5 kDa band (Figure 3C) could have been due to difficulty recovering that fragment from HPLC or due to a cross-link within it. To address both possibilities, we employed an alternate digestion protocol. LysC selectively cleaves the C-terminal to lysine residues and should generate the longer 1−16 fragment of Aβ from a noncovalent dimer. When the four-step purified, gel-extracted ∼8.5 kDa Aβ species is analyzed in this way, the 1−16 fragment is observed, along with the 17−28 and methionine35-oxidized 29−40 fragments (Figure 3D; Table 2; and Figure S2, Supporting Information), thus confirming the identity of the purified ∼8.5 kDa band as a noncovalently linked dimer of Aβ1−40. It is important to note that the sort of MALDI-TOF MS used here is not quantitative; it demonstrates the presence of dimers formed from Aβ1−40 but does not provide information about their abundance.

**Purified Aβ Dimer from 7PA2 Medium Inhibits LTP in Vivo.** To confirm that the bona fide Aβ dimers purified from 7PA2 medium (above) perturb synapse physiology, the purified dimer was tested for its ability to inhibit LTP in vivo upon intracerebroventricular microinjection in healthy adult rats. This *icv* approach was taken because it requires only small sample volumes (≤10 μL) and because we have previously shown that injection of both whole 7PA2 CM and dimer-rich SEC fractions thereof disrupt LTP.[2,4] High frequency stimulation (HFS) of the hippocampal Schaffer collateral pathway fibers in rats that had received the vehicle resulted in the expected induction of LTP that persisted for the course of the experiment (145 ± 10% at 3 h post-HFS relative to baseline EPSP amplitude) (Figure 3E, black). In contrast, when rats were injected with the purified Aβ dimer (of estimated concentration between 0.25 and 2.5 pM), a marked and statistically significant


dx.doi.org/10.1021/bi5003053 | *Biochemistry* 2014, 53, 3908−3921

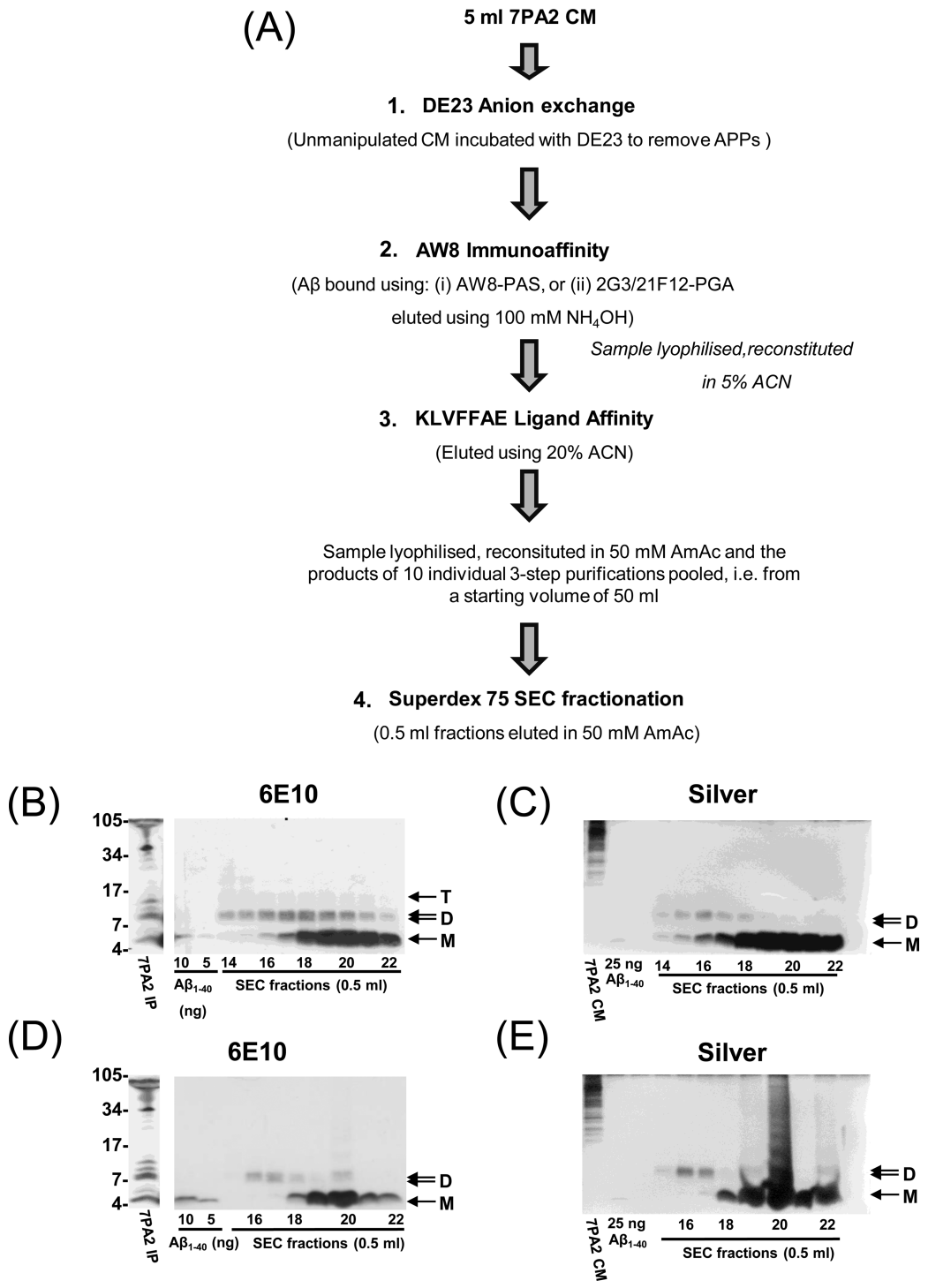


**Figure 2.** Multistep protocol for the purification of cell-derived, soluble A$\beta$ monomers and dimers. (A) The flowchart illustrates the order of individual chromatographic steps. Steps 1−3 were carried out sequentially in batch mode, beginning with 5 mL of 7PA2 CM. The products of 10 such 3-step experiments were then pooled and used for the final SEC fractionation (step 4). Results for experiments using AW8 for immunocapture are shown in B and C, and those using 2G3/21F12 are shown in D and E. (B and D) Final SEC fractions were lyophilized and analyzed by Western blot using 6E10 (30% of each 0.5 mL fraction) and silver stain (60% of each 0.5 mL fraction). The first lane in B and D is an AW8 IP of the starting (unmanipulated) 7PA2 CM, whereas the first lane in C and E is a direct load of 20 $\mu$L of the same CM. The indicated amounts of synthetic A$\beta$1−40 were loaded to allow estimation of the amount of A$\beta$ recovered in the SEC fractions. M, D, and T denote the position where putative A$\beta$ monomer, dimer, and trimer species migrate, and the migrations of molecular weight standards (in kDa) are indicated on the left.

decrease in the EPSP amplitude was observed (103 ± 3%, $p < 0.05$ at 3 h post-HFS) (Figure 3E, red). These results clearly demonstrate that a purified, cell-derived A$\beta$ dimer confirmed by mass spectrometry inhibits LTP in vivo at subnanomolar concentrations in the absence of other factors.

**7PA2 Cells Also Secrete A$\beta$-Immunoreactive Peptides That Lack a Free Asp1 N-Terminus.** The above purification and mass spectrometry indicate the presence of bona fide A$\beta$ dimers in the 7PA2 medium. However, the fact that the putative A$\beta$ trimer in the CM does not copurify with monomer and dimer


dx.doi.org/10.1021/bi5003053 | *Biochemistry* 2014, 53, 3908−3921

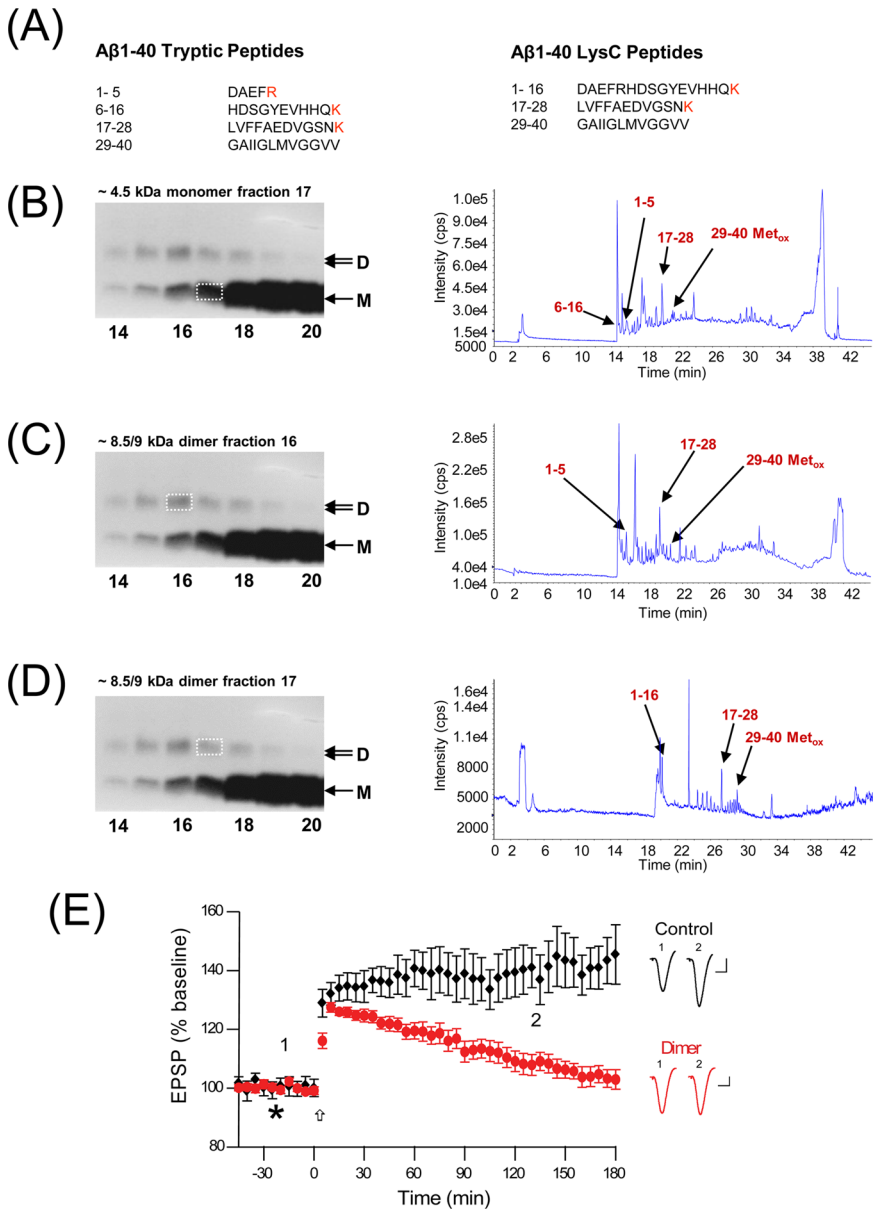


**Figure 3.** MS-confirmed A$\beta$ dimer from 7PA2 CM inhibits LTP in the hippocampus. (A) The single-letter amino acid code of A$\beta$1−40 peptide fragments resulting from digestion using trypsin or LysC. (B−D) Purified 7PA2 CM-derived A$\beta$ obtained using an AW8-PGA affinity conjugate (see Figure 2), and bands corresponding to the ~4.5 kDa monomer or 8.5/9 kDa dimer were excised and subjected to in-gel digestion using trypsin (B−C) or lysC (D). Total ion chromatograms are depicted on the right. Peaks with masses corresponding to A$\beta$1−5, A$\beta$6−16, A$\beta$1−16, A$\beta$17−28, or A$\beta$29−40 are indicated by arrows. Metox. indicates a mass match incorporating oxidized methionine 35. The *Y*-axis on the ion chromatograms represent arbitrary intensity expressed as counts per second (cps). The *X*-axis on the ion chromatograms represent the elution time (min) of components from the Magic C18 AQ column. M and D indicate A$\beta$ monomer and dimer, respectively. (E) Synaptic field potentials were recorded from the CA1 area of anesthetized male Wistar rats. Samples (10 $\mu$L) were injected i.c.v. (*) into healthy adult rats 10 min prior to the induction of LTP by a high-frequency stimulus (HFS). Injection of purified A$\beta$ dimer from 7PA2 CM significantly inhibited LTP (red circles, 103 ± 3% at 3 h post-HFS, $n = 5$, $P < 0.05$) compared to that in the vehicle (black diamonds, 145 ± 10% at 3 post-HFS). Typical EPSPs at (1) ~5 min pre-HFS and (2) ~3 h post-HFS are shown on the right. Statistical comparison of the data was performed on the last 10 min epoch prior to the 3 h time using an unpaired ANOVA. Calibration bars (right) are 10 ms/0.5 mV.

in our 4-step purification and that only one dimer band is purified (Figure 2B and C) whereas a doublet of putative dimers is apparent in unfractionated 7PA2 CM (Figure 1A) suggested that the purified ~8.5 kDa dimer, and the ~9.5 and ~12.5 kDa species have distinct physical properties. Indeed, this supposition is supported by immunochemical results using 3D6, a monoclonal antibody that specifically recognizes the free Asp1 N-terminal residue of A$\beta$ generated by $\beta$-secretase.[29,30] Although 3D6 detects A$\beta$ monomers in SEC fractions 10−11 off of our Superdex 75 column (which correspond to a MW of ~4−5 kDa) and also faintly detects much larger A$\beta$-immunoreactive species (>70 kDa) running natively in the void volume (fractions 5−6), the intermediate soluble species that migrate higher than ~4.5 kDa on SDS−PAGE and occur in SEC fractions 7−9 as detected by 6E10 (Figure 4A, left panel and Figure S2, Supporting Information) are not detectable by 3D6 (Figure 4A, right panels and Figure S2, Supporting Information). The cause of the apparent conflict between the mass spectrometry data on the


dx.doi.org/10.1021/bi5003053 | *Biochemistry* 2014, 53, 3908−3921

**Table 2. LC-MALDI-TOF Detected Fragments Produced by Digestion of Aβ Species Purified from 7PA2 CM[a]**

| sample | peptide | measured mass | theoretical mass$^{(1+)}$ |
|---|---|---|---|
| ~4.5 kDa monomer fraction 17 | 1−5 | 637.3$^{(1+)}$, 319.2$^{(2+)}$ | 636.7 |
| | 6−16 | 1336.2$^{(1+)}$, 668.2$^{(2+)}$ | 1336.4 |
| | 17−28 | 663.3$^{(2+)}$ | 1325.5 |
| | 29−40 $Met_{ox}$ | 1101.6$^{(1+)}$ | 1101.4 |
| ~8.5/9 kDa dimer fraction 16 | 1−5 | 637.3$^{(1+)}$, 319.2$^{(2+)}$ | 636.7 |
| | 17−28 | 663.3$^{(2+)}$ | 1325.5 |
| | 29−40 $Met_{ox}$ | 1101.6$^{(1+)}$ | 1101.4 |
| ~8.5/9 kDa dimer fraction 17 | 1−16 | 489.7$^{(4+)}$, 652.3$^{(3+)}$ | |
| | | 977.9$^{(2+)}$ | 1955.0 |
| | 17−28 | 663.3$^{(2+)}$ | 1325.5 |
| | 29−40 $Met_{ox}$ | 551.3$^{(2+)}$, 1101.6$^{(1+)}$ | 1101.4 |

[a] $Met_{ox}$ = methionine sulfoxide, and $^{(1+)/(2+)/(3+)/(4+)}$ = charge state.

fully purified ~8 kDa species, which confirm the presence of a dimer beginning at Asp1, and the inability to detect this ~8 kDa band with 3D6 on IP/WBs of the total CM is not yet clear. It is possible that the purification procedure facilitated the enrichment of a low-abundance Asp1 dimer that otherwise is not readily detected. In any event, our immunochemical results indicate the presence in CM of low MW Aβ-immunoreactive APP fragments that do not have an exposed (free) Asp1 N-terminus required for the binding of 3D6.

To further examine this possibility, we conducted a series of sequential IP experiments using antibodies raised to various human APP sequences within and flanking the Aβ region. Following each such IP, we then performed a second IP on the residual supernatant using the pan anti-Aβ antiserum, R1282, in order to observe any Aβ-reactive species not brought down by the first IP. All of these samples were Western blotted in parallel with 6E10, an antibody directed to Aβ residues 6−10.[31] Antibodies 4G8 (midregion) and 2G3 ($Aβ_{40}$) plus 21F12 ($Aβ_{42}$) were able to IP both the Aβ monomer and the higher MW bands detectable by 6E10 (Figure 4B). As expected, an antibody raised to the cytoplasmic tail of APP (C8) did not IP any species detectable by 6E10 (Figure 4B). However, pre-β, an antiserum raised to a synthetic peptide of the 20 residues immediately N-terminal to the β-secretase cleavage site (residues 577−596 based on $APP_{695}$ numbering; −1 to −20 relative to Asp1 of Aβ),[8,32] recognized several peptides larger than ~4.5 kDa that appeared to comigrate in part with proteins IP'd by R1282; the pre-β antibody did not detect the monomer (Figure 4B). This unexpected finding suggests that certain species >4.5 kDa recognized by 6E10 are extended N-terminal to the Asp1 of Aβ, consistent with their lack of reactivity with 3D6 (Figure 4A and Figure S3, Supporting Information), which requires a free Asp1 for recognition.[29,30] Importantly, antibodies with similar specificities to 3D6 and pre-β (Table 1) produced highly comparable results. That is, 82E1 (which is specific for Asp1 of Aβ) precipitated only the monomer, and 1G6 (which recognizes an APP sequence ~20 residues N-terminal of Asp1) precipitated peptides between ~8 and 14 kDa but not the monomer (Figure S3, Supporting Information).

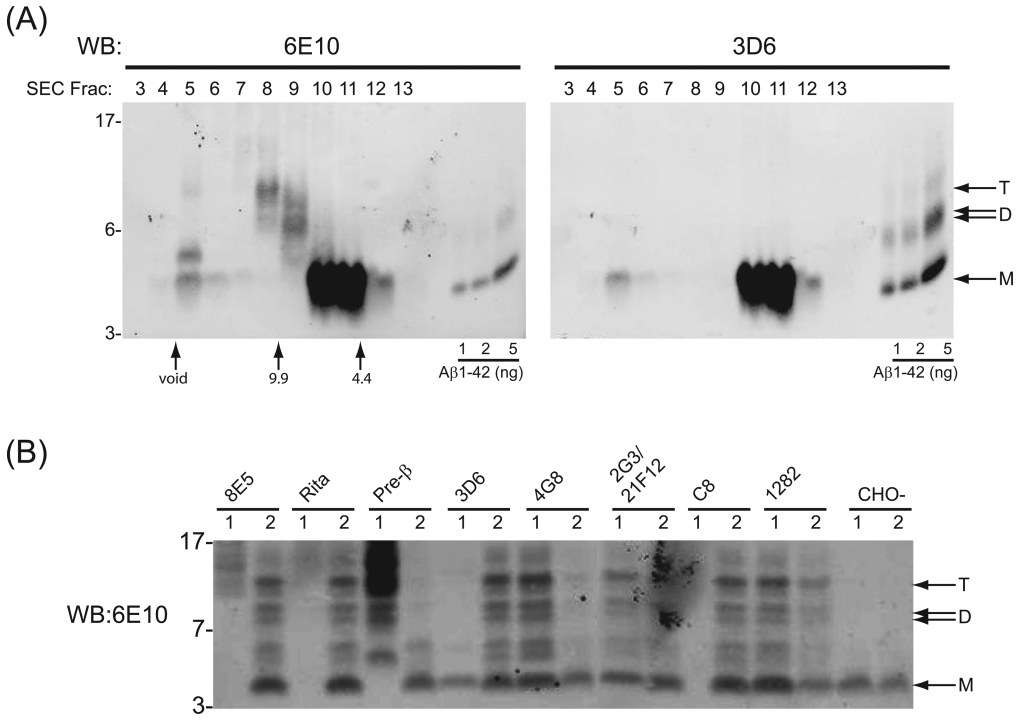


**Figure 4.** The majority of the ~8.5/9 kDa and ~12.5 kDa Aβ-immunoreactive species in 7PA2 CM contain residues N-terminal of Asp1 of Aβ. (A) One milliliter of 10-fold concentrated 7PA2 CM was injected onto a Superdex 75 column and 1 mL fractions collected (#3−13), lyophilized, and equal volumes Western blotted with 6E10 (left panel) or 3D6 (right panel). M, D, and T denote the position where the putative Aβ monomer, dimer, and trimer species migrate, and the migration of PAGE MW standards (kDa) are indicated on the left. Elution of Blue dextran (void) and linear dextran SEC standards of 9.9 and 4.4 kDa are indicated by vertical arrows. (B) 7PA2 CM (2 mL) was first IP'd with the antibody indicated above the lanes labeled 1, and the resultant supernatant was then IP'd with R1282 (lane 2). The polyclonal antibody pre-β, which recognizes APP sequences between residues 577−596 lying N-terminal of Aβ Asp1, precipitated large amounts of 6E10-immunoreactive species and effectively depleted CM of the ~8.5/9 kDa and ~12.5 kDa species otherwise precipitated by R1282. In contrast, the Asp1-specific antibody, 3D6, precipitated only an ~4.5 kDa Aβ monomer leaving most of the putative dimers and trimers to be precipitated by R1282.


dx.doi.org/10.1021/bi5003053 | Biochemistry 2014, 53, 3908−3921

**Two-Dimensional Gel Electrophoresis and Cyanogen Bromide Cleavage Analysis Indicate That the Majority of the Aβ-Immunoreactive ~8.5/9 kDa and ~12.5 kDa Species in 7PA2 CM Have Extended N-Termini.** Because our original radiosequencing of the 7PA2 Aβ oligomers had shown that both the monomer and the putative dimer and trimer bands cut out of one-dimensional gels contained Aβ sequences beginning at Asp1,[8] and because the current mass spectrometry of the purified ~8 kDa dimer band also indicated an Asp1 start site (Figure 3), we used orthogonal biochemical methods to determine whether 7PA2 cells actually secrete a mixture of Aβ-containing species, some that begin at Asp1 and some with N-termini extending "to the left" of Asp1. First, we preformed two-dimensional gel electrophoresis (2DGE) employing isoelectric focusing over a pH range capable of resolving authentic Asp1-initiated Aβ species from N-terminally extended (NTE) Aβ species. To produce a peptide preparation that could be readily solubilized for isoelectric focusing, 7PA2 CM was concentrated, depleted of APPs using DEAE sepharose, and then chromatographed on a Superdex 75 column eluted in a volatile buffer. Fractions 8, 9, and 10 were pooled and then lyophilized to a give a preparation rich in Aβ-immunoreactive species of masses between ~14 and ~4 kDa. This material was then subjected to 2DGE, i.e., isoelectric focusing in the horizontal dimension and denaturing PAGE in the vertical dimension. Once separated in this way, the proteins were transferred onto nitrocellulose, and Aβ-immunoreactive bands were visualized using 6E10. Unexpectedly, only one 6E10-positive spot had an isoelectric point (pI) of ~5.5 close to that expected for Aβ beginning at Asp1, and this migrated in the lithium dodecyl sulfate (LDS)−PAGE dimension at a molecular weight consistent with that of the Aβ monomer (Figure 5A). All of the 6E10-positive bands that migrated on LDS−PAGE with predicted masses ≥6 kDa have pIs less than or equal to 5. Since Aβ peptides beginning at Asp1 and extending to Lys28 and beyond have predicted pIs of ~5.3, and noncovalent oligomers of Aβ1−40 monomers should have the same pI as the monomer, the lack of species larger than the monomer at ~pH 5.3 on our 2D gels indicated that true oligomers are not detected by this method. The fact that the ~8−9 kDa and 12−14 kDa species have pIs ≤5.0 is consistent with these species having NTEs predicted to be ≥34 residues long (ExPASy Proteomics server).

To complement this 2DGE approach, we used cleavage with cyanogen bromide (CNBr) as another means to discriminate between NTE-Aβ and canonical Asp1-starting Aβ species. CNBr cleaves polypeptides on the C-terminal side of methionines. Aβ contains a single Met at position 35, and in the 100 APP residues N-terminal to the Aβ region, there are only 3 Met residues. Fortuitously, one of these is immediately N-terminal of Asp1, and therefore, CNBr cleavage of NTE-Aβ species should liberate Aβ sequences beginning at Asp1. For these experiments, we fractionated 7PA2 CM using SEC and studied the effects of CNBr on the ~4.5 kDa monomer fraction (Frac. 10) vs the ~8−12.5 kDa species (a pool of Frac. 8 and 9) (fraction numbering is as in Figures 1B and 4A). Consistent with our prior results (Figure 4), the SEC-isolated monomer ("Mono −" in Figure 5B) migrates on SDS−PAGE as a single band at ~4.5 kDa before CNBr cleavage and is recognized by 3D6 (indicating its free Asp1 N-terminus), 6E10, and a combination of 2G3 + 21F12 (indicating its free C-termini) but is not recognized by pre-β. Incubation of this material with CNBr ("Mono +" lane in Figure 5B) results in loss of reactivity with 2G3/21F12 and a slightly faster migration of the band detected by 3D6 and 6E10 (Figure 5B). This result is entirely

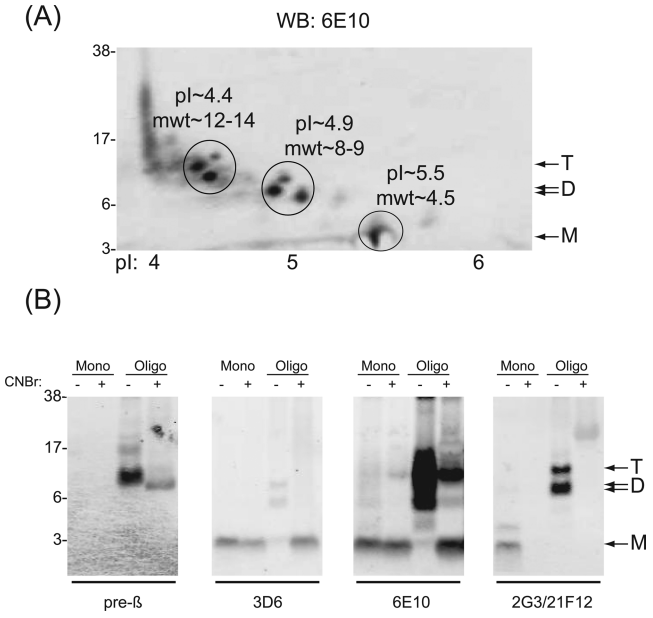


**Figure 5.** Two-dimensional gel electrophoresis and cyanogen bromide cleavage analysis indicate that the majority of the Aβ-immunoreactive ~8.5/9 kDa and ~12.5 kDa species in 7PA2 CM have N-termini that extend beyond Asp1. (A) One milliliter of 10-fold concentrated 7PA2 CM was used for SEC, and fractions rich in Aβ-immunoreactive species of masses between ~14 and ~4 kDa (see Figure 4B) were pooled and used for 2-dimensional gel electrophoresis with immobilized pH 4−7 gradient strips and 4−12% bis-tris gels. 6E10 was used for Western blotting. MW markers were loaded in the well next to the strip, and their migration is indicated on the left; the pH gradient is shown on the bottom. The ~4.5 kDa species migrated with the anticipated pI of Aβ (i.e., ~5.5), whereas the ~8.5/9 kDa and ~12.5 kDa species had lower pI's not compatible with oligomers of Aβ. (B) Ten-fold concentrated 7PA2 CM was fractionated using a Superdex 75 SEC column as described above. Fractions 8−9 were pooled, lyophilized, and designated as the putative oligomer (Oligo) fraction. Monomer-containing fraction 10 (Mono) was lyophilized in a separate tube. The Oligo and Mono samples were incubated overnight in 70% formic acid ± 0.1 M cyanogen bromide (CNBr). Thereafter, samples were electrophoresed on a 12% bis-tris gel and Western blotted. For these experiments, we used a sequential immunoblotting approach: first using pre-β (1st panel) and 2G3/21F12 (4th panel), and then reprobing the pre-β blot with 6E10 (3rd panel) and the 2G3/21F12 blot with 3D6 (2nd panel). CNBr treatment (+) causes a slight down-shift in the migration of the monomer detected by 3D6 and 6E10 and a loss of 2G3/21F12 reactivity, results consistent with cleavage of the monomer after Met35. CNBr treatment of the Oligo fraction (+) leads to the appearance of an ~4 kDa band recognized by 3D6, thus demonstrating that the Oligo fraction contains N-terminally extended Aβ species.

consistent with an Aβ species beginning at Asp1 and extending C-terminal to at least Val40 that loses its C-terminal (2G3/21F12) immunoreactivity after the cleavage by CNBr at Met35 of Aβ. In contrast, the same experiments on the ~8−12.5 kDa species indicated that these species are N-terminally extended beyond Asp1. For example, SEC fractions 8 and 9 contain little 3D6-reactive species before CNBr ("Oligo −" in Figure 5B), but after CNBr ("Oligo +") treatment, a new and prominent 3D6-immunoreactive ~4 kDa band has been generated. Similarly, CNBr treatment markedly alters the species detectable by 6E10, i.e., it drastically reduced the amount of ~6−18 kDa species and produced a new ~4 kDa band. These CNBr cleavage experiments, together with our 2DGE (Figure 5A) and immunoprofiling (Figure 4B), clearly demonstrate that the majority of ~8.5−12.5 kDa Aβ-immunoreactive


dx.doi.org/10.1021/bi5003053 | Biochemistry 2014, 53, 3908−3921

species in the 7PA2 CM are NTE-A$\beta$ species and not oligomers of A$\beta$ monomers beginning at Asp1.

**$\beta$-Secretase Inhibition Increases the Levels of N-Terminally Extended A$\beta$-Containing Peptides in the 7PA2 CM.** To examine the nature of the proteolytic processing of APP that could generate NTE-A$\beta$ species, 7PA2 cells were conditioned in the presence of $\beta$- or $\gamma$-secretase inhibitors. In cells treated with DAPT (a well-characterized $\gamma$-secretase inhibitor[33,34]) all of the bands in the lower gel region normally detected by 6E10, including the A$\beta$ monomer, were decreased or not present in the CM, confirming that all of these A$\beta$-containing species are dependent on $\gamma$-secretase processing, as expected (Figure 6A). Compound IV, a $\beta$-secretase inhibitor,[35] decreased the generation of the ~4.5 kDa A$\beta$ monomer, as expected, but significantly increased the levels of the 6E10 (Figure 6A) and pre-$\beta$ (Figure 6B) reactive species (migrating from ~5 to ~15 kDa), when compared to vehicle-treated (DMSO) cells. Importantly, a similar increase was evident when other potent BACE-specific inhibitors such as Compound III[36] (Figure S4, Supporting Information), Dr9,[37] or Merck compound 3[35] (not shown) were used. These inhibitor effects are consistent with other recent studies on 7PA2 CM[21] and demonstrate that some 6E10-positive species migrating above the monomer are generated by alternative proteolytic processing of APP that increases when $\beta$-secretase-mediated production of the monomer is pharmacologically inhibited.

To examine further the apparent lack of involvement of $\beta$-secretase in generating certain 6E10-reactive APP fragments migrating above the ~4.5 kDa monomer, we stably transfected parental CHO cells with APP constructs bearing single amino acid substitutions within the $\beta$-secretase cleavage region. The Flp-In transfection system was used to ensure equal expression of each APP construct. Lys595Asn and Met596Leu missense mutations in APP occur together in a Swedish kindred with early onset AD,[38] and this mutant precursor undergoes enhanced cleavage by $\beta$-secretase to generate more A$\beta$ monomers than wild type (wt) APP does.[39−41] Consistent with the above BACE inhibitor findings, these Swedish mutations preserve A$\beta$ monomer generation but decrease the amounts of 6E10-reactive species >4.5 kDa (Figure 6C). Conversely, expression of an artificial Met596Val mutation that we previously found to sharply decrease $\beta$-secretase cleavage of APP[42] lowers the production of the A$\beta$ monomer, as expected, but substantially increases the generation of larger A$\beta$-immunoreactive species (Figure 6C). These reciprocal findings, coupled with the BACE inhibitor results (Figure 6A and B), indicate that the majority of the A$\beta$-immunoreactive species detected by 6E10 above ~4.5 kDa do not arise from $\beta$-secretase processing, explaining their lack of reactivity with 3D6 (Asp1-specific).

The findings with the two $\beta$-secretase inhibitors used in Figure 6 and Figure S4 (Supporting Information) were confirmed by a pre-$\beta$ IP of the CM from similarly treated 7PA2 cells: BACE inhibition increased the secretion of species precipitable by pre-$\beta$, whereas DAPT decreased most of these species (Figure 6B). Of note, certain species IP'd by pre-$\beta$ that migrate between ~8 and 14 kDa and are detected by 6E10 are not altered by $\gamma$-secretase inhibition, suggesting that a portion of the bands detected by pre-$\beta$ represent a separate class of APP fragments generated by non-$\gamma$-secretase events. Overall, our findings suggest the existence in this cell line of APP cleavage event(s) occurring N-terminal to the canonical $\beta$-secretase site, followed by $\gamma$-secretase cleavage to generate a C-terminus.

**Secreted NTE-A$\beta$ Species Inhibit Hippocampal LTP.** In view of our observation that soluble NTE-A$\beta$ species constitute

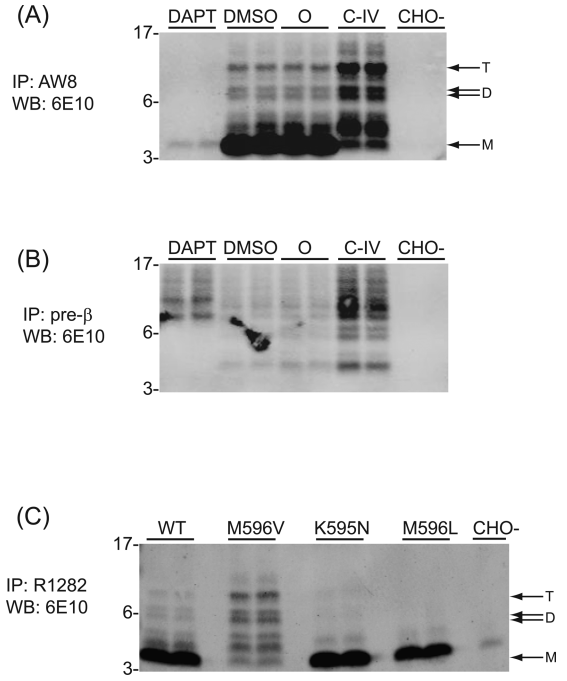


**Figure 6.** $\beta$-Secretase is not necessary for the generation of certain higher MW A$\beta$-immunoreactive species. (A and B) Duplicate dishes of 7PA2 cells were conditioned for ~15 h in the presence or absence of the $\gamma$-secretase inhibitor, DAPT (10 $\mu$M); DMSO vehicle; or the $\beta$-secretase inhibitor, compound IV (3 $\mu$M). CHO- is the CM of parental CHO cells not expressing human APP. CM was collected from cells and used for IP with (A) AW8 and (B) pre-$\beta$, and both Western blotted with 6E10. DAPT treatment of 7PA2 cells blocks the secretion of most species detectable by both R1282 IP and pre-$\beta$ IP. A$\beta$ monomer is significantly reduced in the presence of compound IV (C−IV), but 6E10 immunoreactive species migrating between ~5−16 kDa are increased in quantity. Importantly, certain species IP'd by pre-$\beta$ are still produced in the presence of DAPT, suggesting that these are not products of $\gamma$-secretase activity. (C) Introducing the "Swedish" APP missense mutations (K595N and M596L) increases A$\beta$ monomer levels but decreases levels of the ~5−12.5 kDa 6E10-reactive species relative to CHO cells expressing wtAPP. Conversely, an M596V mutation, which reduces $\beta$-secretase cleavage, decreases A$\beta$ monomers and increases the higher MW species. M, D, and T denote the position where putative A$\beta$ monomer, dimer, and trimer species would migrate, and the migration of MW standards (in kDa) are indicated on the left.

the majority of A$\beta$-immunoreactive species larger than the A$\beta$ monomer in the 7PA2 CM, we asked whether the NTE-A$\beta$ species were also capable of impairing synaptic plasticity. To this end, we performed immunodepletions of either the A$\beta$ oligomers or the NTE-A$\beta$ species from 7PA2 CM, in order to selectively remove A$\beta$ species having either a free Asp1 N-terminus or the N-terminal extensions, respectively. Because the abundant amount of APPs$\alpha$ present in 7PA2 CM could compete with the ability of certain antisera to fully immunodeplete the A$\beta$-NTE species, 7PA2 CM was first incubated with DE23 anion-exchange cellulose to bind and remove the highly charged APPs while leaving the various 4−17 kDa A$\beta$-immunoreactive products in solution. This APP preclearing step generated CM that could then be quantitatively immunodepleted of the NTE species with the pre-$\beta$ antiserum. C8, an antiserum directed to the APP C-terminus, served as a negative control since it did not immunodeplete any of the A$\beta$-containing species found in 7PA2 CM (Figure 4B).

Incubation of 7PA2 CM with PAS and PAG beads in the absence of antibody does not alter the detection of the


dx.doi.org/10.1021/bi5003053 | Biochemistry 2014, 53, 3908−3921

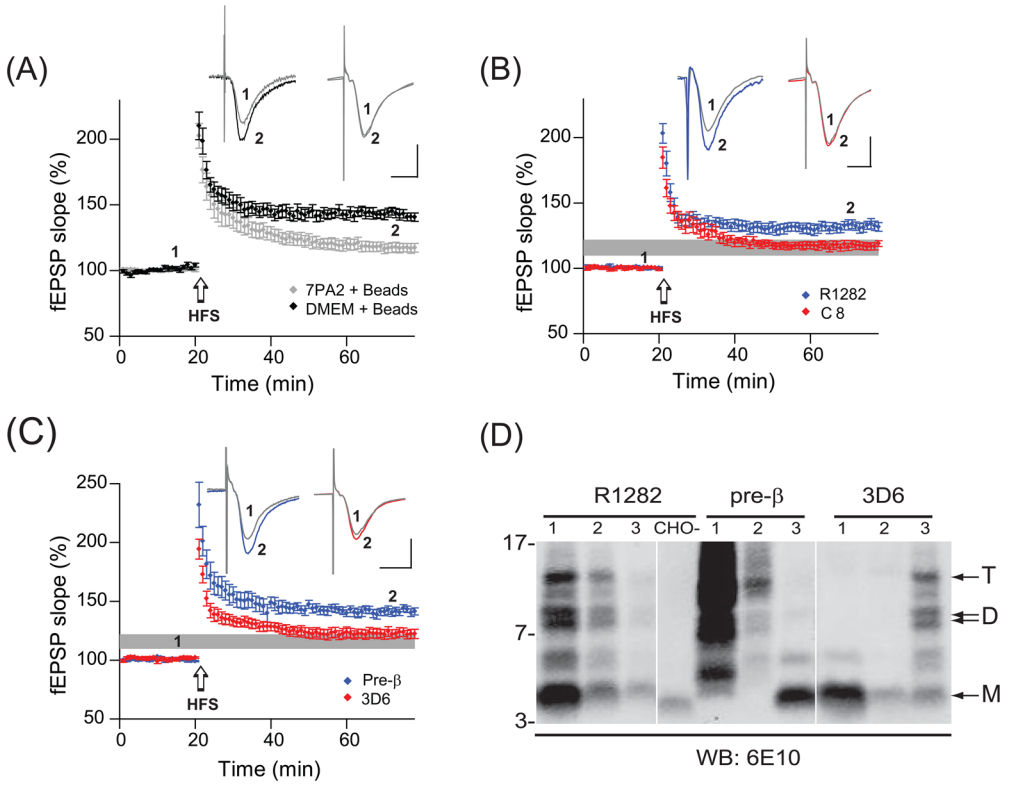


**Figure 7.** N-Terminally extended A$\beta$-containing species in 7PA2 CM inhibit hippocampal LTP. (A) Adult mouse hippocampus slices were exposed to plain DMEM (black) or 7PA2 CM that had been mock-immunodepeleted with antibody-free beads (gray). (B) Immunodepletion with R1282 (blue) significantly decreases the impairment of LTP by 7PA2 CM, whereas immunodepletion with C8 (red) has no effect. The shaded gray horizontal bar represents the mean ±2 SEM of the traces with 7PA2 CM mock-treated with beads shown in A. (C) Immunodepletion of NTE species with pre-$\beta$ (blue) prevents the 7PA2 CM-mediated LTP impairment, but selective removal of only A$\beta$ species starting with a free Asp1 (by antibody 3D6; red) does not significantly decrease the LTP impairment. (D) Western blots of samples IP'd with R1282, pre-$\beta$, and 3D6. Lanes 1 contain precipitates after a first round of IP with the indicated antibody; and lanes 2 contain precipitates after a second round of IP with the same antibody. The supernatant from this second IP was used for LTP analysis in B and C. Lanes labeled 3 are the same supernatants used in B and C that were subsequently IP'd with R1282.

A$\beta$-immunoreactive species IP'd by 1282 (not shown), and consistent with previous observations,[2,9] this negative-control "bead-treated" CM still significantly reduced LTP in adult mouse hippocampus (116.9 ± 3.5% at 60 min, $n$ = 10 slices) compared to that by ACSF supplemented with bead-treated DMEM alone (142.5 ± 3.4%, $n$ = 11 slices; $p < 0.01$) (Figure 7A). Also in accord with our prior work, 7PA2 CM immunodepleted with R1282 no longer impaired LTP (132.4 ± 3.5%, $n$ = 11; $p < 0.01$) compared to that with CM treated with beads alone or immunodepleted with antiserum C8 (117.4 ± 2.8%, $n$ = 8) (Figure 7B,D). Two rounds of immunodepletion of 7PA2 CM with R1282 essentially removed all A$\beta$ peptide containing species between ~4 and 17 kDa (Figure 7D). Immunodepletion of the CM with 3D6 did not significantly rescue LTP (122.4 ± 3.8%, $n$ = 10 $p > 0.05$ for 3D6 compared to beads alone), whereas immunodepletion with pre-$\beta$ did (141.4 ± 3.2%, $n$ = 9; $p < 0.01$ compared to beads alone) (Figure 7C,D). The latter result indicates that the N-terminally extended APP fragments containing the intact A$\beta$ region can impair hippocampal synaptic plasticity, independent of any effects of A$\beta$ oligomers in the CM.

## DISCUSSION

Cultured cells that express mutant human APP and secrete A$\beta$ peptides into their medium have been used to advantage in numerous studies investigating the biological effects of A$\beta$. 7PA2 cells provided the first example of a cell line that secreted A$\beta$-immunoreactive species with biological activity.[2,8] These species migrated on one-dimensional SDS−PAGE gels with molecular weights expected for dimers and trimers were not precipitable with antibodies to flanking APP sequences and showed radiosequencing patterns consistent with A$\beta$ species beginning at Asp1.[8] However, the precise chemical identity of the A$\beta$-immunoreactive species secreted by these cells has not been established heretofore. Consequently, we sought to purify 7PA2-derived ~8.5−12.5 kDa A$\beta$-immunoreactive species to homogeneity (as judged by silver staining), so as to determine their primary sequence (by mass spectrometry) and synaptotoxic potential (by LTP assays).

Using a combination of anion-exchange, immuno-affinity, ligand-affinity, and size-exclusion chromatographies, we successfully purified the ~4.5 and ~8 kDa A$\beta$ species and definitively identified them as monomer and noncovalent dimer, respectively, of A$\beta$1−40. Thereafter, we demonstrated that the purified A$\beta$ dimer from 7PA2 CM, free of other proteins, was sufficient to inhibit LTP in live wt rats. Why the ~12.5 and 9 kDa 6E10-reactive species were not recovered in the purification procedure used to isolate monomer and dimer is unclear. Nonetheless, the preferential loss of these species during purification suggests that they have different physical properties than the monomer and ~8 kDa dimer. Indeed, in preliminary ion-exchange and reverse-phase experiments (not shown), the ~12.5 and 9 kDa species eluted in a fashion that indicated that they are more negatively charged than monomer and dimer and could therefore have distinct primary sequences.


dx.doi.org/10.1021/bi5003053 | *Biochemistry* 2014, 53, 3908−3921

In parallel with our dimer purification efforts, we applied to the 7PA2 CM for the first time an antibody (3D6) uniquely specific for Asp1 of Aβ.[29,30] We observed APP fragments that could be precipitated by pan anti-Aβ antisera (R1282; AW8) and blotted by anti-Aβ monoclonal antibodies that are not Asp1 specific (e.g., 6E10; 4G8) but that could not be detected using 3D6. This unexpected finding led to the experiments herein that demonstrated that NTE-Aβ species are major contributors to the plasticity-disrupting activity of 7PA2 CM. Specifically, certain ∼8−12.5 kDa Aβ-immunoreactive species are recognized by antibodies (pre-β and 1G6) directed to a 20-residue region just N-terminal to the β-secretase cleavage site, and these species migrate on 2D-gels with sizes and pIs consistent with Aβ species with N-terminal extensions >34 residues. Furthermore, treatment of these species with CNBr leads to liberation of the Aβ monomer beginning at Asp1. Most importantly, we present compelling evidence that 7PA2-derived NTE-Aβ fragments impair hippocampal LTP at subnanomolar concentrations and that this synaptotoxic activity is specifically removed by selectively immunodepleting them with the pre-β antiserum.

In view of these new findings, we re-examined our original autoradiograms of IPs that had used pre-β vs anti-Aβ antibodies[8] and confirmed that aliquots of CM of the 7PA2 cell line used at that time (but no longer available) had distinct Aβ-reactive species and pre-β-reactive species whose electrophoretic migration did not overlap on gels or by sequential IPs with the respective antibodies. The most parsimonious explanation for the heterogeneity of Aβ-containing APP fragments that we observe in the present study vs that in 1995 is that the level of β-secretase activity in these non-neural cells changed with cell passage over time. We hypothesize that more recent aliquots of passaged 7PA2 cells have decreased β-secretase levels and/or activity, allowing more APP holoproteins to be processed by alternative proteases which are not inhibited by β-secretase inhibitors and which cleave N-terminal to that Met-Asp site.

Taken together, our previous analyses[8] and those in the current study indicate that 7PA2 cells generate significant amounts of Aβ monomers and NTE-Aβ species (which are also monomeric) as well as small amounts of noncovalent Aβ1−40 dimers. In addition, we also found trace amounts high molecular weight aggregates composed of monomer that eluted in the void volume of a Superdex 75 column. Future studies will be required to determine the relative synaptic potency of the dimers vs the NTE-Aβ's in the 7PA2 CM, but our experiments herein testing the activity of 7PA2 CM immunodepleted with different antibodies indicate that NTE-Aβ's are the primary plasticity-disrupting activity in the current 7PA2 line. Moreover, we present clear pharmacological evidence that the inhibition of BACE leads to an increase in NTE-Aβ's. These findings are consistent with prior studies that tested BACE inhibitors on 7PA2 cells[21] and indicate that at least in CHO cells, APP can be cleaved at sites N-terminal to Asp1 of the Aβ domain by one or more proteases, the action of which are in competition with BACE. Although these alternate species are monomeric APP fragments, they apparently contain a conformation of the Aβ region that confers synaptotoxic effects, as measured by LTP (Figure 7). Comparative studies using soluble Aβ oligomers isolated from the human (AD) cortex or pure, synthetic Aβ show that the electrophysiological effects of these NTE-Aβ monomers are indistinguishable from those of the 7PA2 CM,[12,43] and all 3 sources can also induce AD-type τ hyperphosphorylation and neuritic dystrophy in cultured primary rodent neurons.[43]

We conclude that the heterogeneity of bioactive Aβ-containing species secreted by the 7PA2 cell line makes them a useful source of synaptotoxic Aβ-positive APP fragments, including Aβ dimers, but suggests that any functional effects should be compared to those elicited by human brain-derived or synthetic Aβ dimers. Indeed, given that our previous efforts did not identify Aβ oligomers or NTE-Aβ's in the CM of human neuroblastoma cell lines or primary cortical neurons,[17] it is seems likely that under normal circumstances, neurons do not secrete significant amounts of Aβ oligomers or NTE-Aβ. Nevertheless, there is evidence of alternate NTE-like Aβ-immunoreactive species in human CSF.[44] Consequently, it will be important in future studies to probe other cell culture systems and brain tissues for such NTE-Aβ species, especially to learn whether (as observed here) β-secretase inhibition leads to a rise in the levels of synaptic plasticity-disrupting NTE-Aβ's. The latter phenomenon, if confirmed to occur in vivo, would have important implications for the chronic inhibition of BACE1 in humans.

## ■ ASSOCIATED CONTENT

### Ⓢ Supporting Information

Mass spectrometric analysis of the purified ∼8.5/9 kDa band; 7PA2 CM contains species with the Aβ epitope but without a free Asp1 N-terminus; antibody 1G6 detects 6E10-reactive species that migrate between ∼8−14 kDa; and β-secretase inhibitor reduces the production of Aβ monomer, but increases production of ∼5−16 kDa Aβ immunoreactive species. This material is available free of charge via the Internet at http://pubs.acs.org.

## ■ AUTHOR INFORMATION

### Corresponding Authors

*(D.M.W.) E-mail: dwalsh3@partners.org.

*(D.J.S.) E-mail: dselkoe@partners.org.

### Author Contributions

#A.T.W., J.E.M., and G.M.S. contributed equally to this work.

### Funding

The research leading to these results received funding from the European Community's Seventh Framework Programme (FP7/2007-2013) under Grant Agreement No. 200611 (to D.M.W.) and was supported by NIH grants IRO1AGO27443 (to D.M.W. and D.J.S.), 1R01AG01673 (to D.J.S.), and by the Foundation for Neurologic Diseases (to D.J.S.). A.T.W. was funded by a European Union 6th Framework Marie Curie Early Stage Training fellowship.

### Notes

The authors declare no competing financial interest.

## ■ ACKNOWLEDGMENTS

We thank Dr. David Scopes for the gift of the KLVFFAE-Ac-HN-$(CH_2)$3-CPG beads, Dr. Ron Wang for sharing unpublished data, Ms. Nina Shepardson for technical assistance, and Drs. Marcia B. Podlisny and Jessica M. McDonald for useful discussions.

## ■ ABBREVIATIONS

Aβ, amyloid β-protein; ACN, acetonitrile; ACSF, artificial cerebrospinal fluid; AD, Alzheimer's disease; BACE, β-amyloid cleaving enzyme-1; Buffer A, 20 mM ammonium acetate at pH 8.5; CHO, Chinese hamster ovary cells; CM, conditioned medium; 2DGE, two-dimensional gel electrophoresis; DMEM, Dulbecco's modified Eagle's medium; EDTA, Ethylenediaminetetraacetic acid; EPSP, excitatory postsynaptic potential; fEPSP,

field excitatory postsynaptic potential; *icv*, intracerebroventricular; IP, immunoprecipitation; IPG, immobilized pH gradient; LC, liquid chromatography; LTP, long-term potentiation; MALDI-TOF MS, matrix-assisted laser desorption/ionization-time-of-flight mass spectrometry; NTE, N-terminal extension; 7PA2, Chinese hamster ovary cells stably expressing human $APP_{751}$ bearing the V717F mutation; PAGE, polyacrylamide gel electrophoresis; PAS, protein A sepharose; PGA, protein G agarose; PBS, phosphate buffered saline; PBST, phosphate buffered saline plus 0.05% (v/v) Tween 20; PCR, polymerase chain reaction; pI, isoelectric point; RT, room temperature; S/LDS−PAGE, sodium/lithium dodecyl sulfate−polyacrylamide gel electrophoresis; SEC, size-exclusion chromatography; STEN, 50 mM Tris at pH 7.4 containing 2 mM EDTA, 0.2% NP40, and 650 mM NaCl; TBS, tris-buffered saline; TBST, tris-buffered saline plus 0.05% (v/v) Tween 20

## REFERENCES


(1) Lambert, M. P., Barlow, A. K., Chromy, B. A., Edwards, C., Freed, R., Liosatos, M., Morgan, T. E., Rozovsky, I., Trommer, B., Viola, K. L., Wals, P., Zhang, C., Finch, C. E., Krafft, G. A., and Klein, W. L. (1998) Diffusible, nonfibrillar ligands derived from Abeta1−42 are potent central nervous system neurotoxins. *Proc. Natl. Acad. Sci. U.S.A. 95*, 6448−6453.

(2) Walsh, D., Klyubin, I., Fadeeva, J., Cullen, W., Anwyl, R., Wolfe, M., Rowan, M., and Selkoe, D. (2002) Naturally secreted oligomers of the Alzheimer amyloid $\beta$-protein potently inhibit hippocampal long-term potentiation *in vivo*. *Nature 416*, 535−539.

(3) Gong, Y., Chang, L., Viola, K. L., Lacor, P. N., Lambert, M. P., Finch, C. E., Krafft, G. A., and Klein, W. L. (2003) Alzheimer's disease-affected brain: presence of oligomeric A beta ligands (ADDLs) suggests a molecular basis for reversible memory loss. *Proc. Natl. Acad. Sci. U.S.A. 100*, 10417−10422.

(4) Klyubin, I., Walsh, D. M., Lemere, C. A., Cullen, W. K., Shankar, G. M., Betts, V., Spooner, E. T., Jiang, L., Anwyl, R., Selkoe, D. J., and Rowan, M. J. (2005) Amyloid beta protein immunotherapy neutralizes Abeta oligomers that disrupt synaptic plasticity in vivo. *Nat. Med. 11*, 556−561.

(5) Lesne, S., Koh, M. T., Kotilinek, L., Kayed, R., Glabe, C. G., Yang, A., Gallagher, M., and Ashe, K. H. (2006) A specific amyloid-beta protein assembly in the brain impairs memory. *Nature 440*, 352−357.

(6) Calabrese, B., Shaked, G. M., Tabarean, I. V., Braga, J., Koo, E. H., and Halpain, S. (2007) Rapid, concurrent alterations in pre- and postsynaptic structure induced by naturally-secreted amyloid-beta protein. *Mol. Cell Neurosci. 35*, 183−193.

(7) Shankar, G. M., Li, S., Mehta, T. H., Garcia-Munoz, A., Shepardson, N. E., Smith, I., Brett, F. M., Farrell, M. A., Rowan, M. J., Lemere, C. A., Regan, C. M., Walsh, D. M., Sabatini, B. L., and Selkoe, D. J. (2008) Amyloid-beta protein dimers isolated directly from Alzheimer's brains impair synaptic plasticity and memory. *Nat. Med. 14*, 837−842.

(8) Podlisny, M. B., Ostaszewski, B. L., Squazzo, S. L., Koo, E. H., Rydel, R. E., Teplow, D. B., and Selkoe, D. J. (1995) Aggregation of secreted amyloid beta-protein into SDS-stable oligomers in cell culture. *J. Biol. Chem. 270*, 9564−9570.

(9) Townsend, M., Shankar, G. M., Mehta, T., Walsh, D. M., and Selkoe, D. J. (2006) Effects of secreted oligomers of amyloid beta-protein on hippocampal synaptic plasticity: a potent role for trimers. *J. Physiol. 572*, 477−492.

(10) Shankar, G. M., Bloodgood, B. L., Townsend, M., Walsh, D. M., Selkoe, D. J., and Sabatini, B. L. (2007) Natural oligomers of the Alzheimer amyloid-beta protein induce reversible synapse loss by modulating an NMDA-type glutamate receptor-dependent signaling pathway. *J. Neurosci. 27*, 2866−2875.

(11) Bate, C., and Williams, A. (2011) Amyloid-beta-induced synapse damage is mediated via cross-linkage of cellular prion proteins. *J. Biol. Chem. 286*, 37955−37963.

(12) Li, S., Hong, S., Shepardson, N. E., Walsh, D. M., Shankar, G. M., and Selkoe, D. (2009) Soluble oligomers of amyloid Beta protein facilitate hippocampal long-term depression by disrupting neuronal glutamate uptake. *Neuron 62*, 788−801.

(13) Cleary, J. P., Walsh, D. M., Hofmeister, J. J., Shankar, G. M., Kuskowski, M. A., Selkoe, D. J., and Ashe, K. H. (2005) Natural oligomers of the amyloid-beta protein specifically disrupt cognitive function. *Nat. Neurosci. 8*, 79−84.

(14) Poling, A., Morgan-Paisley, K., Panos, J. J., Kim, E. M., O'Hare, E., Cleary, J. P., Lesne, S., Ashe, K. H., Porritt, M., and Baker, L. E. (2008) Oligomers of the amyloid-beta protein disrupt working memory: confirmation with two behavioral procedures. *Behav. Brain Res. 193*, 230−234.

(15) Freir, D. B., Fedriani, R., Scully, D., Smith, I. M., Selkoe, D. J., Walsh, D. M., and Regan, C. M. (2011) Abeta oligomers inhibit synapse remodelling necessary for memory consolidation. *Neurobiol. Aging 32*, 2211−2218.

(16) Kittelberger, K. A., Piazza, F., Tesco, G., and Reijmers, L. G. (2012) Natural amyloid-beta oligomers acutely impair the formation of a contextual fear memory in mice. *PLoS One 7*, e29940.

(17) Walsh, D. M., Tseng, B. P., Rydel, R. E., Podlisny, M. B., and Selkoe, D. J. (2000) Detection of intracellular oligomers of amyloid $\beta$-protein in cells derived from human brain. *Biochemistry 39*, 10831−10839.

(18) Shankar, G. M., Welzel, A. T., McDonald, J. M., Selkoe, D. J., and Walsh, D. M. (2011) Isolation of low-n amyloid beta-protein oligomers from cultured cells, CSF, and brain. *Methods Mol. Biol. 670*, 33−44.

(19) Shevchenko, A., Wilm, M., Vorm, O., and Mann, M. (1996) Mass spectrometric sequencing of proteins silver-stained polyacrylamide gels. *Anal. Chem. 68*, 850−858.

(20) Koo, E. H., and Squazzo, S. L. (1994) Evidence that production and release of amyloid beta-protein involves the endocytic pathway. *J. Biol. Chem. 269*, 17386−17389.

(21) Portelius, E., Olsson, M., Brinkmalm, G., Ruetschi, U., Mattsson, N., Andreasson, U., Gobom, J., Brinkmalm, A., Holtta, M., Blennow, K., and Zetterberg, H. (2013) Mass spectrometric characterization of amyloid-beta species in the 7PA2 cell model of Alzheimer's disease. *J. Alzheimer's Dis. 33*, 85−93.

(22) Walsh, D. M., Klyubin, I., Fadeeva, J. V., Rowan, M. J., and Selkoe, D. J. (2002) Amyloid-beta oligomers: their production, toxicity and therapeutic inhibition. *Biochem. Soc. Trans. 30*, 552−557.

(23) Xia, W., Zhang, J., Kholodenko, D., Citron, M., Podlisny, M. B., Teplow, D. B., Haass, C., Seubert, P., Koo, E. H., and Selkoe, D. J. (1997) Enhanced production and oligomerization of the 42-residue amyloid beta-protein by Chinese hamster ovary cells stably expressing mutant presenilins. *J. Biol. Chem. 272*, 7977−7982.

(24) Galeazzi, L., Ronchi, P., Franceschi, C., and Giunta, S. (1999) In vitro peroxidase oxidation induces stable dimers of beta-amyloid (1−42) through dityrosine bridge formation. *Amyloid 6*, 7−13.

(25) Al-Hilaly, Y. K., Williams, T. L., Stewart-Parker, M., Ford, L., Skaria, E., Cole, M., Bucher, W. G., Morris, K. L., Sada, A. A., Thorpe, J. R., and Serpell, L. C. (2013) A central role for dityrosine crosslinking of Amyloid-beta in Alzheimer's disease. *Acta Neuropathol. Commun. 1*, 83.

(26) O'Malley, T. T., Oktaviani, N. A., Zhang, D., Lomakin, A., O'Nuallain, B., Linse, S., Benedek, G. B., Rowan, M. J., Mulder, F. A., and Walsh, D. M. (2014) Abeta dimers differ from monomers in structural propensity, aggregation paths, and population of synaptotoxic assemblies, *Biochem. J.*, DOI: 10.1042/BJ20140219.

(27) Ikura, K., Takahata, K., and Sasaki, R. (1993) Cross-linking of a synthetic partial-length (1−28) peptide of the Alzheimer beta/A4 amyloid protein by transglutaminase. *FEBS Lett. 326*, 109−111.

(28) Hartley, D. M., Zhao, C., Speier, A. C., Woodard, G. A., Li, S., Li, Z., and Walz, T. (2008) Transglutaminase induces protofibril-like amyloid beta-protein assemblies that are protease-resistant and inhibit long-term potentiation. *J. Biol. Chem. 283*, 16790−16800.

(29) Miles, L. A., Crespi, G. A., Doughty, L., and Parker, M. W. (2013) Bapineuzumab captures the N-terminus of the Alzheimer's disease amyloid-beta peptide in a helical conformation. *Sci. Rep. 3*, 1302.

(30) Feinberg, H., Saldanha, J. W., Diep, L., Goel, A., Widom, A., Veldman, G. M., Weis, W. I., Schenk, D., and Basi, G. S. (2014) Crystal structure reveals conservation of Aβ conformation recognized by 3D6 following humanization to bapineuzumab, *J. Alzheimer's Dis.*, in press.
(31) Currie, J. R., Ramakrishna, N., Burrage, T. G., Hwang, M. C., Potempska, A., Miller, D. L., Mehta, P. D., Kim, K. S., and Wisniewski, H. M. (1991) Immunolocalization of Alzheimer β-amyloid peptide precursor to cellular membranes in baculovirus expression system. *J. Neurosci Res. 30*, 687−698.
(32) Estus, S., Golde, T. E., Kunishita, T., Blades, D., Lowery, D., Eisen, M., Usiak, M., Qu, X. M., Tabira, T., Greenberg, B. D., et al. (1992) Potentially amyloidogenic, carboxyl-terminal derivatives of the amyloid protein precursor. *Science 255*, 726−728.
(33) Yagishita, S., Morishima-Kawashima, M., Tanimura, Y., Ishiura, S., and Ihara, Y. (2006) DAPT-induced intracellular accumulations of longer amyloid beta-proteins: further implications for the mechanism of intramembrane cleavage by gamma-secretase. *Biochemistry 45*, 3952−3960.
(34) Dovey, H. F., John, V., Anderson, J. P., Chen, L. Z., de Saint Andrieu, P., Fang, L. Y., Freedman, S. B., Folmer, B., Goldbach, E., Holsztynska, E. J., Hu, K. L., Johnson-Wood, K. L., Kennedy, S. L., Kholodenko, D., Knops, J. E., Latimer, L. H., Lee, M., Liao, Z., Lieberburg, I. M., Motter, R. N., Mutter, L. C., Nietz, J., Quinn, K. P., Sacchi, K. L., Seubert, P. A., Shopp, G. M., Thorsett, E. D., Tung, J. S., Wu, J., Yang, S., Yin, C. T., Schenk, D. B., May, P. C., Altstiel, L. D., Bender, M. H., Boggs, L. N., Britton, T. C., Clemens, J. C., Czilli, D. L., Dieckman-McGinty, D. K., Droste, J. J., Fuson, K. S., Gitter, B. D., Hyslop, P. A., Johnstone, E. M., Li, W. Y., Little, S. P., Mabry, T. E., Miller, F. D., and Audia, J. E. (2001) Functional gamma-secretase inhibitors reduce beta-amyloid peptide levels in brain. *J. Neurochem. 76*, 173−181.
(35) Stachel, S. J., Coburn, C. A., Steele, T. G., Jones, K. G., Loutzenhiser, E. F., Gregro, A. R., Rajapakse, H. A., Lai, M. T., Crouthamel, M. C., Xu, M., Tugusheva, K., Lineberger, J. E., Pietrak, B. L., Espeseth, A. S., Shi, X. P., Chen-Dodson, E., Holloway, M. K., Munshi, S., Simon, A. J., Kuo, L., and Vacca, J. P. (2004) Structure-based design of potent and selective cell-permeable inhibitors of human beta-secretase (BACE-1). *J. Med. Chem. 47*, 6447−6450.
(36) Tung, J. S., Davis, D. L., Anderson, J. P., Walker, D. E., Mamo, S., Jewett, N., Hom, R. K., Sinha, S., Thorsett, E. D., and John, V. (2002) Design of substrate-based inhibitors of human beta-secretase. *J. Med. Chem. 45*, 259−262.
(37) Ghosh, A. K., Kumaragurubaran, N., Hong, L., Kulkarni, S., Xu, X., Miller, H. B., Reddy, D. S., Weerasena, V., Turner, R., Chang, W., Koelsch, G., and Tang, J. (2008) Potent memapsin 2 (beta-secretase) inhibitors: design, synthesis, protein-ligand X-ray structure, and in vivo evaluation. *Bioorg. Med. Chem. Lett. 18*, 1031−1036.
(38) Mullan, M., Crawford, F., Houlden, H., Axelman, K., Lilius, L., Winblad, B., and Lannfelt, L. (1992) A pathogenic mutation for probable Alzheimer's disease in the APP gene at the N-terminus of β-amyloid. *Nat. Genet. 1*, 345−347.
(39) Citron, M., Oltersdorf, T., Haass, C., McConlogue, L., Hung, A. Y., Seubert, P., Vigo-Pelfrey, C., Lieberburg, I., and Selkoe, D. J. (1992) Mutation of the β-amyloid precursor protein in familial Alzheimer's disease increases β-protein production. *Nature 360*, 672−674.
(40) Cai, X.-D., Golde, T. E., and Younkin, G. S. (1993) Release of excess amyloid β protein from a mutant amyloid β protein precursor. *Science 259*, 514−516.
(41) Citron, M., Vigo-Pelfrey, C., Teplow, D. B., Miller, C., Schenk, D., Johnston, J., Winblad, B., Venizelos, N., Lannfelt, L., and Selkoe, D. J. (1994) Excessive production of amyloid β-protein by peripheral cells of symptomatic and presymptomatic patients carrying the Swedish familial Alzheimer's disease mutation. *Proc. Natl. Acad. Sci. U.S.A. 91*, 11993−11997.
(42) Citron, M., Teplow, D. B., and Selkoe, D. J. (1995) Generation of amyloid β-protein from its precursor is sequence specific. *Neuron 14*, 661−670.
(43) Jin, M., Shepardson, N., Yang, T., Chen, G., Walsh, D., and Selkoe, D. J. (2011) Soluble amyloid beta-protein dimers isolated from Alzheimer cortex directly induce Tau hyperphosphorylation and neuritic degeneration. *Proc. Natl. Acad. Sci. U.S.A. 108*, 5819−5824.
(44) Portelius, E., Brinkmalm, G., Tran, A. J., Zetterberg, H., Westman-Brinkmalm, A., and Blennow, K. (2009) Identification of novel APP/Abeta isoforms in human cerebrospinal fluid. *Neurodegener. Dis. 6*, 87−94.
(45) McConlogue, L., Castellano, F., deWit, C., Schenk, D., and Maltese, W. A. (1996) Differential effects of a Rab6 mutant on secretory versus amyloidogenic processing of Alzheimer's beta-amyloid precursor protein. *J. Biol. Chem. 271*, 1343−1348.
(46) Kim, K. S., Wegiel, J., Sapienza, V., Chen, J., Hong, H., and Wisniewski, H. M. (1997) Immunoreactivity of presenilin-1 in human, rat and mouse brain. *Brain Res. 757*, 159−163.
(47) Johnson-Wood, K., Lee, M., Motter, R., Hu, K., Gordon, G., Barbour, R., Khan, K., Gordon, M., Tan, H., Games, D., Lieberburg, I., Schenk, D., Seubert, P., and McConlogue, L. (1997) Amyloid precursor protein processing and A beta42 deposition in a transgenic mouse model of Alzheimer disease. *Proc. Natl. Acad. Sci. U.S.A. 94*, 1550−1555.
(48) Haass, C., Schlossmacher, M. G., Hung, A. Y., Vigo-Pelfrey, C., Mellon, A., Ostaszewski, B. L., Lieberburg, I., Koo, E. H., Schenk, D., Teplow, D. B., et al. (1992) Amyloid beta-peptide is produced by cultured cells during normal metabolism. *Nature 359*, 322−325.
(49) McDonald, J. M., Savva, G. M., Brayne, C., Welzel, A. T., Forster, G., Shankar, G. M., Selkoe, D. J., Ince, P. G., Walsh, D. M., Medical Research Council Cognitive, F., and Ageing, S. (2010) The presence of sodium dodecyl sulphate-stable Abeta dimers is strongly associated with Alzheimer-type dementia. *Brain 133*, 1328−1341.